R. & M. No. 3175
(20,502)
A.R.C. Technical Report

R. & M. No. 3175

MINISTRY OF AVIATION

AERONAUTICAL RESEARCH COUNCIL
REPORTS AND MEMORANDA

The Steady Flow of a Viscous Fluid Past a Circular Cylinder at Reynolds Numbers 40 and 44

By C. J. APELT

LONDON: HER MAJESTY'S STATIONERY OFFICE
1961
PRICE 11*s.* 0*d.* NET

The Steady Flow of a Viscous Fluid Past a Circular Cylinder at Reynolds Numbers 40 and 44

By C. J. Apelt

of the Department of Engineering Science, University of Oxford

Reports and Memoranda No. 3175
October, 1958

Summary. This paper describes the numerical solution of the complete Navier-Stokes equations for the steady flow of an incompressible viscous fluid of unlimited extent past a circular cylinder at Reynolds number 40. A new device developed for the numerical solution is described. The results of the investigation are:

(*a*) A steady-state solution does exist at Reynolds number 40 and is in good agreement with experimental results.

(*b*) It seems that steady-state solutions are possible for somewhat higher Reynolds numbers even though they may not exist in nature. A solution has been obtained at Reynolds number 44 but it has not been carried to the same accuracy as the solution at Reynolds number 40.

(*c*) The length of the stationary vortex pair attached to the downstream portion of the cylinder continues to increase with Reynolds number in such steady-state solutions up to a Reynolds number 44 and no indication has been found that this process will not continue as the Reynolds number is increased beyond 44.

1. *Introduction.* The attention which the problem of the steady flow of a viscous fluid past a circular cylinder at low Reynolds numbers has received seems rather less than the theoretical interest of the problem would lead one to expect. This, no doubt, is partly due to the complexity of the equations governing such motions. The first attempts to study this problem used some approximate and apparently reasonable assumptions to simplify the Navier-Stokes equations. Thus the Stokes approximation to these equations, which consists in the omission of the inertial terms as having negligible significance in flows at very low Reynolds numbers, reduces the two-dimensional form of the equations to

$$\nabla^4\psi = 0\,. \tag{1}$$

The solution for the steady flow of a viscous fluid past a sphere by means of the three-dimensional form of Stokes's equation is well known. However, both Stokes and Lamb[1] have pointed out that if the attempt is made to find the steady motion produced by the translation of a cylinder with constant velocity through a liquid of infinite extent on the basis of the equation (1) it is impossible to satisfy all the conditions. It seems that no steady 'creeping flow' of a viscous fluid past an infinite cylinder is possible. Bairstow, Cave and Lang[2] found it possible to obtain a definite resistance for the circular cylinder in 'creeping flow' if it is placed in a channel having parallel walls.

If the equations of motion are approximated after the manner of Oseen, in which the inertia terms are partially taken into account, a definite value is obtained for the resistance of the cylinder in a stream of infinite extent. The solution is given by Lamb (loc. cit.). However, this solution is valid only for small values of the Reynolds number and in addition, as Lamb points out, with the Oseen equations the boundary conditions are only approximately satisfied. In a second paper Bairstow, Cave and Lang[3] developed the solution of Lamb and extended it to cover larger values of the Reynolds number. They claim their solution extends to a Reynolds number of approximately 25 but even at a Reynolds number of 10 the value they obtained for the coefficient of drag is 31 per cent higher than the value obtained experimentally. They suggested, moreover, that they had made the maximum possible use of the Oseen approximation to the equations for viscous flow past a cylinder. Tomotika and Aoi[4] have also used the Oseen approximation to calculate the flow past a circular cylinder for the range of Reynolds numbers 0·05 to 4.

The first successful attempt at a solution of the complete Navier-Stokes equations for viscous flow past a circular cylinder was made by Thom[5]. By means of a numerical process similar in essentials to that described below, he obtained numerical solutions at Reynolds numbers 10 and 20. His calculated values for the drag of the cylinder are in good agreement with experimental results. More recently, Kawaguti[6] has obtained a solution at Reynolds number 40 by a numerical method based on that of Thom, and Allen and Southwell[7] have published relaxation solutions for Reynolds numbers 0 (sic!), 1, 10, 100 and 1000.

The present work is concerned with the numerical solution of the complete Navier-Stokes equations for steady flow past a circular cylinder at Reynolds number 40. It is worth recording here why it was decided to proceed with an independent solution at this Reynolds number even though Kawaguti had already obtained a solution. It is a fact shown by experimental results (*e.g.*, Refs. 5 and 8) that as the Reynolds number of the flow past a circular cylinder is increased the pair of stationary vortices attached to the rear of the cylinder increases in length in the direction of the flow until the steady regime breaks down and the Kármán vortex street develops at a Reynolds number of about 40 (Ref. 9). Kawaguti's solution at Reynolds number 40 shows that the length of the vortex pair had increased over that in Thom's solution at Reynolds number 20. There seemed to be no obvious reason why this process of the lengthening of the standing vortices should not continue for solutions at Reynolds numbers greater than 40 though such steady state solutions may not exist in nature at these higher values of Reynolds number. However, in the solutions published by Allen and Southwell the length of the vortex pair at Reynolds number 100 was less than that in Kawaguti's solution at Reynolds number 40 and it decreased further when the Reynolds number was increased from 100 to 1000.

It was considered important to resolve this apparent contradiction. The solution was undertaken for a Reynolds number of 40 because of Kovasznay's hypothesis that 'the critical Reynolds number at which the vortex street sets in is a well-defined value' which in his experiments was 40 (Ref. 9). This suggested that if the steady-state solution of the Navier-Stokes equations did in fact throw any light on the problem of the critical Reynolds number it would do so at or about this value. Moreover, experience with numerical solutions of viscous flow in a suddenly expanding channel suggested that the region to be studied in greatest detail should be the wake for a considerable distance downstream of the cylinder. The transformation which Kawaguti employed for his solution, illustrated in Fig. 1, was such that the whole region of the wake external to a radius of five times the

cylinder radius was covered by two intervals of the mesh and at the infinity points he had imposed a definite 'infinity condition'.

It was decided, therefore, to proceed with a solution having greater detail in the wake downstream of the cylinder. Further, no assumption was made concerning conditions at very great distance from the cylinder, except that as the distance from the cylinder increased the flow would tend more and more to the uniform stream. To implement these decisions entailed a very great increase in the work required for a numerical solution, but it was considered important to obtain a solution, the validity of which could be accepted with as few reservations as possible.

Initially the number of difficulties encountered seemed to preclude the feasibility of a steady-state solution under these conditions but eventually after a very great amount of labour the many difficulties were resolved and the solution presented below was obtained. In general, it agrees quite closely with that of Kawaguti in the region near the cylinder but there are considerable differences in the region of the wake at large distances from the cylinder. After the solution at Reynolds number 40 had been completed a solution at Reynolds number 44 was also obtained though not to the same accuracy as that of the former, since it was considered of interest only in so far as it confirmed certain conclusions deduced from the solution at Reynolds number 40.

As a result of this investigation it can be stated that:

(*a*) A steady-state solution of the Navier-Stokes equations does exist for a Reynolds number of 40, and it is in good agreement with experimental results.

(*b*) Further, a steady-state solution does exist for Reynolds number 44 and experience with the two solutions gives good reason to expect that such steady-state solutions are possible at higher Reynolds numbers, though the labour of this form of numerical solution is likely to increase very much as the Reynolds number increases, because of the greater development of the wake.

(*c*) There is no reason to expect that the tendency of the standing vortex pair to increase in length downstream as the Reynolds number increases will be reversed at any stage; it seems that the solutions of Allen and Southwell which do show this tendency to have been reversed may be distorted through the use of too coarse a mesh for the numerical calculations.

After this investigation was completed, Payne[10] published solutions for the starting flow of a viscous fluid past a circular cylinder at Reynolds numbers 40 and 100. The starting flow is, of course, a different problem from the final steady-state flow and direct comparison between the results of the present investigation and those of Payne is not possible. However, his results for the starting flow at Reynolds number 40 seem generally consistent with the results obtained here for the final steady-state and it seems that the unsteady flow pattern would approach more and more closely the steady-state solution if it were carried on for longer times.

2. *Equations of Motion and Boundary Conditions.* In this investigation we consider the steady flow of an incompressible viscous fluid of unlimited extent past an infinitely long circular cylinder. The fluid is taken as flowing in the positive direction of x with a velocity in the undisturbed stream of U'. The radius of the cylinder is L'.

The Navier-Stokes equations, which describe this motion, are solved in the form:

$$\nabla^2\zeta = \frac{R}{2}\left(\frac{\partial\psi}{\partial x}\frac{\partial\zeta}{\partial y} - \frac{\partial\psi}{\partial y}\frac{\partial\zeta}{\partial x}\right) \tag{2}$$

$$\nabla^2\psi = \zeta\,, \tag{3}$$

where

$$\nabla^2 \equiv \left(\frac{\partial^2}{\partial x^2} + \frac{\partial^2}{\partial y^2}\right)$$

and $R \equiv 2U'L'/\nu'$ is the Reynolds number based on the diameter of the cylinder. ν' is the kinematic viscosity of the fluid. The stream function ψ is defined by

$$u = -\frac{\partial \psi}{\partial y}, \quad v = \frac{\partial \psi}{\partial x} \tag{4}$$

and the vorticity ζ is defined by

$$\zeta = \frac{\partial v}{\partial x} - \frac{\partial u}{\partial y}. \tag{5}$$

These equations have been given in their non-dimensional form. Unprimed symbols are dimensionless whereas primed symbols are dimensional. The dimensional and dimensionless quantities are related to each other as follows:

$$\left.\begin{aligned} &x' = L'x, \quad y' = L'y, \quad u' = U'u, \quad v' = U'v, \quad q' = U'q \\ &X' = \frac{U'^2}{L'}x, \quad p' = (\tfrac{1}{2}\rho' U'^2)p \\ &\psi' = U'L'\psi, \quad \zeta' = \frac{U'}{L'}\zeta \end{aligned}\right\}, \tag{6}$$

where x, y, u, . . . , etc., are dimensionless variables corresponding to x', y', u', . . . , etc.

At the boundary of the cylinder the conditions to be satisfied are that no fluid may cross the solid boundary and that there is no 'slipping' at the surface of the cylinder. These boundary conditions may be expressed

$$\frac{\partial \psi}{\partial x} = 0 = \frac{\partial \psi}{\partial y}. \tag{7}$$

As the distance from the cylinder becomes very large it is assumed that the flow will approach more and more to the uniform stream, *i.e.*,

$$\psi \to -y, \quad \zeta \to 0.$$

The use of the Navier-Stokes equations in the form given above enables ζ and ψ to be calculated on separate but inter-related fields and each calculation is concerned with an equation of the second order. This approach is far simpler than attempting to calculate ψ directly by the single fourth-order equation obtained by combining the equations (2) and (3). Further, in the 'double-field' method the numerical solution has a much faster rate of convergence than does a process based on the single fourth-order equation.

3. *Transformation from the Physical Plane.* The numerical solution of this problem is to be effected on a square mesh covering the field of flow and to avoid the complication of 'irregular stars' at the curved boundary of the cylinder use is made of a transformation from the physical plane as first demonstrated by Thom[5]. The equations of motion are solved in the transformed, $\alpha\beta$ plane

$$t = \alpha + i\beta, \tag{8}$$

which is connected to the physical, xy plane,

$$z = x + iy = re^{i\theta} \tag{9}$$

by a conformal transformation

$$t = f(z) . \tag{10}$$

The equations of motion are transformed to

$$\nabla^2_{\alpha\beta}\zeta = \frac{R}{2}\left(\frac{\partial\psi}{\partial\alpha}\frac{\partial\zeta}{\partial\beta} - \frac{\partial\psi}{\partial\beta}\frac{\partial\zeta}{\partial\alpha}\right) \tag{2a}$$

$$\nabla^2_{\alpha\beta}\psi = \frac{\zeta}{M^2}, \tag{3a}$$

where

$$\nabla^2_{\alpha\beta} = \left(\frac{\partial^2}{\partial\alpha^2} + \frac{\partial^2}{\partial\beta^2}\right)$$

and M is the modulus of transformation.

The transformation employed here is

$$t = ki \log z = ki \log (re^{i\theta}) ,$$

so that

$$\alpha = -k\theta$$

$$\beta = k \log r ,$$

and

$$M^2 = \left(\frac{\partial\beta}{\partial x}\right)^2 + \left(\frac{\partial\beta}{\partial y}\right)^2 = \left(\frac{\partial\beta}{\partial r}\right)^2 = \left(\frac{k}{r}\right)^2 .$$

The transformation is illustrated in Fig. 2. k has been taken as $20/\pi$ giving twenty mesh points to the half cylinder. Since the flow is symmetrical about the x axis only half the field of flow need be considered. The lower half of the xy plane external to the cylinder ($\infty > r > 1$, $0 > \theta > -\pi$) is transformed into the semi-infinite slot ($0 < \alpha < 20$, $0 < \beta < \infty$).

This transformation, in addition to avoiding irregular stars at the surface of the cylinder, has the further advantage that a uniform mesh in the transformed plane represents a system of radiating lines and concentric circles in the physical plane, giving smaller squares near the cylinder where greater detail is required and increasingly larger squares further out without, however, compressing the details of the wake as does the transformation illustrated in Fig. 1.

4. *Numerical Solution.* For the purpose of numerical solution the differential equations (2*a*), (3*a*) are approximated to by finite difference equations and values of the functions ζ, ψ are computed at the discrete points of a rectangular mesh in the $\alpha\beta$ plane (Fig. 2b). The simplest finite difference approximations to the equations (2*a*), (3*a*) are respectively:

$$\zeta_0 = \zeta_m - \frac{R}{32}[(a - c)(B - D) + (b - d)(C - A)] \tag{11}$$

$$\psi_0 = \psi_m - \frac{n^2\zeta_0}{2M^2}, \tag{12}$$

which are the formulae used by Thom[5] in his solution at Reynolds number 20. In these equations ζ_0 is the value of ζ at the centre of a square of side $2n$, recalculated from the corner values, and ζ_m is

the mean of these corner values. The small letters in the equation (11) represent ζ values and capital letters ψ values at the mesh points as shown in Fig. 3a.

It was found that more powerful devices than the simple application of the equations (11) and (12) had to be developed for the solution at Reynolds number 40 and these devices are described below.

5. *Finite Difference Approximations to the Boundary Conditions.* At the solid boundary of the cylinder ψ is known and is constant. The values of ζ at the boundary must be calculated from the pattern of flow in the immediate vicinity of the boundary. The method of solution, essentially, is to calculate the values of ζ, ψ in the flow for certain assumed values of ζ at the boundary. Boundary values of ζ are then recalculated from these new values of ζ and ψ in the flow and the sequence is continued until the boundary values repeat themselves to the required degree of accuracy. The finite difference formula used for calculation of the boundary values of ζ must incorporate the boundary conditions given above, equation (7). That used here is due to Woods[11],

$$\zeta_0 = \frac{3M_0^2}{h^2}(\psi_1 - \psi_0) - \frac{1}{2}\frac{M_0^2}{M_1^2}\zeta_1 , \tag{13}$$

where ζ_0 is the boundary value and ζ_1, ψ_1 are values at a point in the flow distant h from the boundary (Fig. 3b).

There are circumstances in which the use of the equation (13) fails to achieve convergence as has been pointed out in Ref. 12. In this solution the mesh size near the boundary was made very much smaller than the critical mesh size given in Ref. 12 to avoid any difficulties arising from divergence at the boundary. Further, the rate of convergence was considerably increased by the following simple device: the new values of ζ_0 at the boundary, given by the equation (13), were not used directly for the next sequence of calculations but rather the mean of the previous and the newly recalculated values was used as the boundary value for the next sequence.

6. *Procedure of Solution and Special Devices.* At first the method of solution was kept as routine as possible in an endeavour to ascertain whether the problem (or a similar one) could be solved by a technique suitable for programming for an electronic computer.

The first trial values for ζ, ψ were based partly on Kawaguti's solution, in the region between mesh lines $\beta = 0$ and $\beta = 5$, and partly on an approximate extrapolation from Thom's solution for Reynolds number 20, in the region $\beta > 5$. The equations (11), (12) and (13) were employed to improve the assumed values of ζ and ψ at each point of the mesh and on the boundary in turn. It soon became obvious that it was not possible to obtain a solution in this manner and divergence of the process began to occur in the field beyond $\beta = 4$ ($r = 1{\cdot}874$). The analysis of this difficulty has been described in Ref. 12, and there a new device is developed whereby a definite portion only of the movement of ζ, as determined by the local field configuration, is added at each stage of the calculations. This device was used in this problem and in this way the area in which the solution could be accomplished was considerably extended (as far as $\beta = 10$, $r = 4{\cdot}810$ approximately) but the device was not powerful enough for the region of the wake beyond $\beta = 10$. Eventually use had to be made of every device available including the one just referred to and a second new device described below.

The final technique developed is as follows:

When divergence occurs it appears first in the calculation of ζ and so the maximum effort must be devoted to the calculation of this function. The equation (3*a*) for ψ is linear and gives rise to no special difficulties.

(i) In general, the values of ζ and ψ were improved separately over the whole field or large sections of it since it was found that attempts at improving their values simultaneously at each point gave rise to violent fluctuations.

(ii) In the inner region, $0 < \beta < 8$, the values of ζ were first improved by means of the device developed in Ref. 12 and referred to above. This consisted in taking the new value of ζ_0 for use in the next cycle of calculations as

$$\zeta_{0\,\mathrm{new}} = \frac{\zeta_{0r} + b\zeta_{0i}}{1 + b}, \tag{14}$$

where $\zeta_{0\,\mathrm{new}}$ is the improved value of ζ_0 to be used in the next cycle, ζ_0 is the previous value, and ζ_{0r} is the value recalculated by the equation (11) from the values of ζ at surrounding points. The optimum value of b at each point can be shown to be (*cf.*, Ref. 12),

$$b = \left(\frac{R}{32}\right)^2 [(E - G)^2 + (F - H)^2] - \tfrac{1}{4}, \tag{15}$$

where the letters $E, \ldots H$ represent the values of ψ at the corresponding points in Fig. 3a. The value of b changes as the field pattern alters. However, it was found to alter so slowly that it was necessary to recalculate it only infrequently.

(iii) Later, as the solution was improved the values ζ_{0r} in this region, $0 < \beta < 8$, were recalculated from the formula, due to Bickley[13]

$$\zeta_0 = \frac{4S_1 + S_2}{20} - \frac{6l^2\nabla^2_{\alpha\beta}\zeta_0}{20} - \frac{l^4\nabla^4_{\alpha\beta}\zeta_0}{40}, \tag{16}$$

where

$$S_1 = a + b + c + d$$

$$S_2 = e + f + g + h,$$

the small letters representing the values of ζ at the corresponding points in Fig. 3a. The formula (16) is more accurate than (11), the neglected terms being $0(l^6)$. In the present context the equation (16) becomes

$$\zeta_0 = \frac{4S_1 + S_2}{20} - 6l^2J - \tfrac{1}{2}l^4\nabla^2_{\alpha\beta}J, \tag{16a}$$

where

$$J \equiv \left(\frac{\partial\psi}{\partial\alpha}\frac{\partial\zeta}{\partial\beta} - \frac{\partial\psi}{\partial\beta}\frac{\partial\zeta}{\partial\alpha}\right).$$

Initially J was approximated to by the simple finite difference formula,

$$J = \frac{1}{4l^2}[(a - c)(B - D) + (b - d)(C - A)], \tag{17}$$

which appears in the equation (11). As the solution proceeded this approximation also was improved by use of Bickley's '5-point' differentiation formula[14] for the calculation of each differential in the expression for J, e.g.,

$$\left(\frac{\partial\zeta}{\partial\alpha}\right)_0 \doteq \frac{1}{12l}\left[\zeta_Z - 8\zeta_D + 8\zeta_B \to \zeta_K\right]. \tag{18}$$

The value of $\nabla^2_{\alpha\beta}J$ for use in the formula (16a) was obtained at each point by the formula

$$\nabla^2_{\alpha\beta}J = \frac{4S_1' + S_2' - 20J_0}{6l^2}, \tag{19}$$

where

$$S_1' = J_A + J_B + J_C + J_D$$

$$S_2' = J_E + J_F + J_G + J_H. \quad \text{(Fig. 3a).}$$

This formula was found accurate enough for the calculation of $\nabla^2_{\alpha\beta}J$ for the effect of this term in the equation (16a), though important, was small relative to the term in J itself by a ratio which varied in value from one tenth to one fifth.

(iv) For the region of the wake, $\beta > 8$, a new device had to be developed for the improving of the value of ζ. The device combines features of Thom's numerical method and of the relaxation type of technique. It was found important in this solution to keep in view at all times the actual values of ζ, ψ, and so the approach was to work with the values of ζ, ψ, rather than with 'residuals'. For this region of the field an 'operation pattern' was prepared showing the effect on the value of ζ at neighbouring points of a unit change in the value of ζ at each point. One 'molecule' of this 'operation pattern' is illustrated in Fig. 4. In general the coefficients at each point differ from each other and each molecule is different. Strictly, since the calculation of ζ_0 is based, in this region, on the equations (16a), (18) and (19), each molecule should show effects at the twelve surrounding points shown in Fig. 4, from a change in the value of ζ at the central point. However, at the points connected by dotted lines the coefficients are small compared to those at the inner four points and it was found sufficient in practice to use the simplified four-point molecule. Further, it was found that $\nabla^2_{\alpha\beta}J$ varied rather more slowly than did J and ζ and in the preparation of the 'operation pattern' it was found possible to ignore the effect of the term in $\nabla^2_{\alpha\beta}J$ in the equation (16a). Of course, when the new value of ζ_0 was being recalculated the full equations (16a), (18) and (19) were used taking into account the effect of all twelve points shown in Fig. 4.

The sequence of operations in this region was then, starting from a distribution of ζ, ψ, to calculate the new values of ζ at each point by use of the equations (16a), (18) and (19). These, in general, would differ from the previous values. The 'operation pattern' would then be used to reduce progressively, by adjustments to the ζ field, the total values of 'residuals' in the region, where by 'residual' is meant here the difference between the recalculated value of ζ and the previous value. The 'operation pattern' itself changes with each alteration to the field configuration, but in practice its change was slow enough to enable the one pattern to be used unaltered through several sequences before a new pattern had to be calculated. When the total value of 'residuals' had been reduced to a degree, indicated as appropriate by experience with previous sequences, the new configuration of ψ was calculated from the resulting new configuration of ζ. ζ was then recalculated with the equations (16a), (18) and (19) and the whole process described above was repeated.

In using the 'operation pattern' to reduce the total value of 'residuals' much use was made of block moves, the most powerful ones employed being a movement of the same sign and of approximately the same magnitude in the value of ζ at every point over large sections of the field; sometimes a similar block move but confined to only one α line; and sometimes a combination of two such 'line movements' of opposite sign. The foregoing technique was found to be very powerful in this region of the field. It should be emphasised that at no stage were the newly calculated values of ζ used directly for the fresh start of the next sequence but rather techniques of under-relaxation and over-relaxation were employed as indicated by the configuration of the field. The aim at all times was to reduce the sum of 'residuals' of ζ over large regions and at the same time to reduce the average value of 'residuals' at each point while making them all to be of approximately the same magnitude. At no stage was it attempted to eliminate individual residuals as this approach gave rise to violent fluctuations in the values at surrounding points. This is illustrated by the fact that in this region a unit movement at a single point can alter 'residuals' at surrounding points by ten times its own value and more. Adjustments to the ζ configuration in this area must be made with great care, but there is the compensating advantage that quite small irregularities are immediately indicated by violent fluctuations in the values of ζ at surrounding points.

(v) Distant points: The desire to avoid the imposition of an 'infinity' condition at points which are in fact at a finite distance has been mentioned above. It is obvious that the calculations cannot be carried to such a distance that the infinity conditions could be applied directly and the difficulty was overcome in the following way.

Far down in the wake ($\beta > 20$, $r > 23 \cdot 14$), ζ is confined to a narrow region and it was found possible to extrapolate the configuration of ζ beyond any given stage in the calculation quite closely. The technique was, at each stage, to extrapolate the value of ζ for four mesh lines beyond the limits of the previous cycle of calculations. The whole sequence of recalculation of ψ and adjustment of ζ as described in sections (i) to (iv) above was then carried out for this enlarged area. The process of extrapolation was then used to extend the area another four mesh lines and the whole sequence was repeated. This technique proved quite effective. It was found unnecessary to extend the calculations further than $\beta = 30$ ($r = 111 \cdot 3$) for, provided the field in this distant region was approximately correct, refinements to it did not appreciably affect the solution closer in to the cylinder.

The extrapolation of ζ in this distant region could be achieved quite closely because if its rate of decrease was made too great the next cycle of calculation made values of ζ closer in to increase very much and vice versa as illustrated in Fig. 5. This enabled the extrapolated values of ζ to be fixed quite closely by preliminary calculations in the immediate locality before the full-scale recalculation described above was undertaken. In such preliminary calculations use was made of a device, illustrated in Fig. 6, which was developed independently but which had been used earlier in different contexts by Green[15] and by Thom[16]. The recalculated value, ζ_n, was plotted against the previous trial value, ζ_{n-1}, for three or four cycles and the value where the curve joining these points intersected the line, $\zeta_n = \zeta_{n-1}$, was taken for the next trial value of ζ. This device had to be employed with a degree of caution but it was found to speed the solution in this distant region of the wake.

(vi) ψ: The treatment of ψ needs no special mention except that for ψ in the region where ζ is zero much use was made of the graded mesh (which is not convenient for use with ζ); also of the 'large squares' formulae and of the method of 'differences' due to Thom[17]. The important thing to note about ψ is that the residuals of ψ have an importance approximately inversely proportional to

the distance from the cylinder and for $\beta < 12$ an extra decimal place was preserved in the calculation of ψ. On the other hand the residuals of ζ are important wherever ζ exists but more especially in the region of the wake.

(vii) Finally, as an overall check on the validity of the extrapolation of ζ far out and also as a check on the overall correctness of the field, at intervals in the solution integrals for the drag force on the cylinder were calculated at a number of circles, usually at those corresponding to $\beta = 10$ ($r = 4{\cdot}810$) and $\beta = 14$ ($r = 9{\cdot}017$), and the results were compared with the drag force obtained by integration round the surface of the cylinder itself. This is discussed in more detail in the Appendix I dealing with the accuracy of the solution.

7. *Summarised Procedure of Calculation.* The final technique developed for the solution of this problem was as summarised below:

(1) With the field configuration of ζ, ψ at any given stage as the result of a completed sequence, ζ was extrapolated four mesh lines further

(2) This extrapolation was then improved as described in Section 6 (v)

(3) The pattern of ψ was then recalculated over the whole field

(4) The boundary values of ζ were adjusted as indicated by the equation (13)

(5) The 'operation pattern' of Section 6 (iv), was adjusted if necessary and the values of ζ in the field were improved by the method appropriate to the region (*cf.*, Sections 6 (ii) to 6 (iv))

(6) The extrapolation of ζ was carried a stage further and the whole sequence (1) to (5) repeated.

The sequence should not be regarded as a rigid routine because at times, depending on how the field was behaving, one or more steps were omitted or carried out over only a portion of the field.

8. *Results.* The values obtained for ψ and ζ in the region $0 \leqslant \beta \leqslant 20$ for Reynolds number 40 are given in Appendices II and III respectively. Even when all the devices described above are employed the process of solution is long and laborious and no claim is made that the numerical results of Appendices II and III are absolutely final. It is considered, however, that further refinement would result in only slight changes in the numerical results presented here. The accuracy of the solution is discussed at greater length in a later section (*Note:* The numerical results given in the Appendices II and III are for the lower half of the physical plane, the calculations having been performed for this half of the plane. However, for convenience of comparison with other results all the diagrams and discussions of the remainder of Section 8 relate to the flow in the upper half of the physical plane).

8.1. *Flow Pattern.* From the numerical results for ψ given in Appendix II contours of ψ have been plotted to give the pattern of streamlines near the cylinder, shown in Fig. 7. The pattern is in very good agreement with that shown by photographs of flows at comparable Reynolds numbers (*cf.*, Refs. 5, 8, 18 and 19). In particular comparison should be made with the photographs at Reynolds numbers 41 and 42 given in Ref. 19. Referring now to Fig. 7, it will be seen that the stationary vortex pair attached to the cylinder is very prominent and has increased considerably in length over that obtained by Thom[5] in his numerical solution at Reynolds number 20. It is also

somewhat longer than the vortex pair in Kawaguti's solution at the same Reynolds number, *i.e.*, 40 (Ref. 6). It is suggested that this difference is probably due to the transformation this latter author employed (Fig. 1) which greatly compresses the area of the wake and possibly caused small distortions in his solution in this region. It will also be remarked that even at a distance of 6·5 radii downstream of the cylinder (the limit of the extent of Fig. 7), the streamlines in the body of the flow have scarcely begun to close up again behind the cylinder, indicating the increased development of the wake.

8.2. *Vorticity.* Contours of vorticity, plotted from the results of Appendix III are shown in Fig. 8. The vorticity will be seen to persist for a very long way downstream of the cylinder. Another feature of Fig. 8 is the existence of an area in the main body of the flow where the vorticity changes sign. It was expected, of course, that the vorticity would change sign in the region of the vortex pair but in the main body of the flow a change of sign was not permitted during the earlier stages of the solution. However, in the region of Fig. 8 where the second area of small positive vorticity occurs, positive residuals of ζ recurred persistently and could be eliminated only by allowing ζ there to take on small positive values. It is possible, on the other hand, that this area of small positive vorticity is caused by truncation errors in the numerical solution, a point which could be investigated by further subdivision of the mesh on which the solution is calculated.

The distribution of vorticity on the surface of the cylinder is shown in Fig. 9. Points scaled from the corresponding curve presented by Kawaguti are also shown plotted in Fig. 9 and the two results are very similar. Even though there are differences between the present solution and that of Kawaguti at increasing distances from the cylinder (chiefly in that in this solution the vorticity spreads much farther downstream in the wake), the solutions are in close agreement for the region near the cylinder. This constitutes further justification for the hypothesis put forward in an earlier Section that reasonably small inaccuracies in the solution at great distances from the cylinder do not appreciably affect the solution close in.

8.3. *Velocity Distribution in the Wake.* Velocity profiles calculated in the wake downstream of the cylinder are shown in Fig. 10. The series of profiles illustrates how the wake gradually decreases in intensity and spreads laterally with increasing distance from the cylinder. Experimental results obtained by Kovasznay[9] at Reynolds number 34 with hot-wire anemometer measurements are also plotted in Fig. 10. Near the cylinder the profiles are quite similar but there are increasing differences further downstream, indicating the greater development of the wake as the Reynolds number increases from 34 to 40.

8.4. *Pressure Distribution on the Cylinder.* The Navier-Stokes equations can be integrated to give equations for determining the difference in pressure at points in the fluid. In the present context they were used in the form

$$p_B - p_A = q_A^2 - q_B^2 + \frac{4}{R}\int_A^B \frac{\partial \zeta}{\partial \alpha}\, d\beta + 2\int_B^A \zeta \frac{\partial \psi}{\partial \beta}\, d\beta \tag{20}$$

for integration between points A and B on a line $\alpha = \text{const}$ in the $\alpha\beta$ plane, and

$$p_D - p_C = q_C^2 - q_D^2 - \frac{4}{R}\int_C^D \frac{\partial \zeta}{\partial \beta}\, d\alpha + 2\int_C^D \zeta \frac{\partial \psi}{\partial \alpha}\, d\alpha \tag{21}$$

for integration between points C and D on a line $\beta = \text{const}$.

The pressure on the front generator of the cylinder was obtained with the equation (20) by integration along the line $\alpha = 20$. The value obtained is $1 \cdot 154$. Thom[5] found experimental values at Reynolds numbers 36 and 45 of $1 \cdot 19$ and $1 \cdot 16$ respectively. Kawaguti's theoretical value at Reynolds number 40 was $1 \cdot 142$. Thom's approximate theory for determining the value of the pressure on the front generator at low speeds[20] gives the result at Reynolds number 40, $(1 + 7/R)$ or $1 \cdot 175$, which is still a fairly good approximation.

The pressure at other points on the cylinder was obtained by integration along the line, $\beta = 0$, by means of the equation (21). The values obtained are given in Table 1, and they have been plotted to give the pressure distribution shown in Fig. 11. Also plotted in Fig. 11 are Thom's experimental results at Reynolds numbers 36 and 45 and points from Kawaguti's calculated curve for Reynolds number 40. The results of the present solution lie, on the whole, between the experimental results for the higher and lower Reynolds number. Kawaguti's results do not differ by much from the present results but they tend to lie wholly above both sets of experimental results.

TABLE 1

θ (deg)	$p_\theta = \frac{p'_0 - p'_\infty}{\frac{1}{2}\rho' U'^2}$
Upstream stagnation point 180	$+1 \cdot 15_5$
162	$0 \cdot 85$
144	$+0 \cdot 13$
126	$-0 \cdot 61$
108	$-1 \cdot 00_5$
90	$-1 \cdot 04_5$
72	$-0 \cdot 92_5$
54	$-0 \cdot 78$
36	$-0 \cdot 66_5$
18	$-0 \cdot 58_5$
0 Downstream stagnation point	$-0 \cdot 55_5$

8.5. *Drag on the Cylinder.* The drag force on the cylinder can be obtained from the calculated pressure and vorticity distributions on its surface by the equation

$$\text{Drag per unit length} = -2\int_0^\pi p_{(r=1)} \cos\theta \, d\theta - \frac{4}{R}\int_0^\pi \zeta_{(r=1)} \sin\theta \, d\theta \,, \tag{22}$$

where the drag is in non-dimensional form, $(\text{Force}/\frac{1}{2}\rho' U'^2)$.

The result is expressed as a coefficient

$$C_D = (\text{Drag force per unit length})/\tfrac{1}{2}\rho' U'^2(2L')$$
$$= C_{Dp} + C_{Df}.$$

The first term of the right-hand side of the equation (22) leads to C_{Dp}, the value obtained being 0·928. This is lower than Kawaguti's value of 1·053 but is in good agreement with Thom's experimental results. For Reynolds numbers 36 and 45 he found C_{Dp} to have the values 0·98 and 0·92 respectively. The second term of the right-hand side of the equation (22) leads to C_{Df} which was calculated at 0·568, which is very close to Kawaguti's figure of 0·565. The total coefficient of drag, C_D, thus has the value 1·496.

In Fig. 12 this result is plotted together with some other theoretical and experimental values of C_D over the range $1 < R < 1000$. The agreement between the value obtained here and experimental results is quite good even though the experimental values at Reynolds number 40 were probably obtained for flows of a periodic nature.

8.6. *Growth of the Stationary Vortex Pair.* In Fig. 13 the length of the stationary vortex pair attached to the cylinder is plotted over the range $1 < R < 1000$. This figure incorporates both theoretical results and values measured from photographs obtained in the range of steady flows by a number of investigators. Despite a certain amount of scattering of the points (due partly to the difficulty of measuring accurately the length of the vortex pair in the photographs available and partly to the effect of the varying proximity of the channel walls on the length of the vortex pair), the experimental results illustrate quite clearly the increase in length of the stationary vortex pair with increase in Reynolds number up to the stage when the steady regime breaks down. The length of the vortex pair obtained in the present investigation at Reynolds number 40, *i.e.*, 2·13 diameters, is in very close agreement with Taneda's[19] experimental result of 2·1 diameters.

In general, all the theoretical results plotted in Fig. 13 are in good agreement with the experimental results with two exceptions, the results of Allen and Southwell[7] for Reynolds numbers of 100 and 1000. The experience with the solution at Reynolds number 40 indicated that it was most unlikely that the vortex pair would not continue to grow in length as the Reynolds number was increased. To confirm this a solution has been obtained at Reynolds number 44. It has not been completed to the same accuracy as that of Reynolds number 40, but it has been taken to a stage where the length of the vortex pair has settled down and is not significantly altered by further refinements of the solution. The length of the vortex pair so obtained at Reynolds number 44 is 2·3, which value is also plotted on Fig. 13, and is in good agreement with the general trend of the other results. No evidence was found that the vortex pair would not continue to grow for higher Reynolds numbers and it is suggested, therefore, that the two anomalous results of Allen and Southwell, in which the vortex pair has diminished in length as the Reynolds number increased from 40 to 1000 may have been obtained on a mesh rather too coarse, resulting in distortions of the solution.

It seems then reasonably certain that for considerable increases in the Reynolds number beyond 44, theoretical solutions will show the vortex pair to continue increasing in length. However, it is difficult to predict what will happen to the vortex pair at very large Reynolds numbers. Imai[23] concluded that the asymptotic flow pattern around a bluff body for viscous flow at vanishing viscosity is a discontinuous flow with a dead water region of the Kirchhoff type. Kawaguti, following Imai,

suggested that as the Reynolds number increased indefinitely the theoretical solution would become similar to that obtained by the discontinuous-flow theory. On the other hand, Batchelor[21] has suggested that the length of the vortex pair will tend eventually to a constant value as the Reynolds number approaches infinity. If the length of the vortex pair is plotted against Reynolds number on a natural scale instead of the logarithmic scale of Fig. 13, it appears that for the higher values of Reynolds number the length of the vortex pair is increasing linearly with Reynolds number, as was observed by Taneda[24]. However, it is not possible to extrapolate beyond the plotted data of Fig. 13 with any degree of confidence. Calculations at Reynolds numbers higher than 44 would seem desirable to throw light on this problem.

8.7. *Breakdown of the Steady-Flow Pattern.* The present solutions having been obtained from the Navier-Stokes equations for steady conditions, they cannot be expected by themselves to give any direct information about the formation of the Kármán vortex street, which is an unsteady state. However, they do show that steady-state solutions are theoretically possible at Reynolds numbers 40 and 44 and it seems that steady-state solutions are possible for even higher Reynolds numbers. This having been established, it is interesting to reconsider the somewhat varied results of experimenters who have observed the onset of the Kármán vortex street in the wake of the circular cylinder. Thus, although Kovasznay claimed that the vortex street sets in at a definite Reynolds number, which in his experiments was 40, Thom[5] found that the critical Reynolds number varied from approximately 30 to 62 as the ratio of channel width to cylinder diameter was varied over the range 40 to 10. Taneda obtained photographs of the stationary vortex pair up to a Reynolds number 57·7 but considered that the critical Reynolds number for the formation of the Kármán vortex street was about 45. Camichel, Dupin and Teissié-Solier[22] observed periodic oscillations in the flow and alternate shedding of vortices at a Reynolds number as low as 23·3, but they found that the fully developed vortex street did not establish itself finally until a Reynolds number of 47.

These disparate results can be reconciled if we postulate that the breakdown of the steady regime and the formation of the Kármán vortex street is a phenomenon of hydrodynamic instability which is affected by a number of factors including the proximity of the channel walls and the degree of turbulence of the main stream. This being so, it is to be expected that the onset of the Kármán vortex street will take place over a range of Reynolds numbers, depending on such factors as mentioned above, and not at any particular value of the Reynolds number.

9. *Conclusion.* The findings of this investigation may be summarised:

(i) A steady state solution of the Navier-Stokes equations for the flow of a viscous fluid past a circular cylinder does exist for Reynolds number 40 and is in good agreement with experimental results.

(ii) Further, a steady state solution exists for Reynolds number 44 and it seems that such solutions are possible for higher Reynolds numbers though the corresponding flow may not exist in nature.

(iii) The length of the stationary vortex pair attached to the cylinder continues to increase with increasing Reynolds number in such theoretical solutions up to a Reynolds number of 44 and there is no indication that this tendency will be reversed as the Reynolds number is increased beyond 44.

(iv) It is postulated that the Reynolds number at which the steady regime breaks down and the Kármán vortex streets sets in will depend on a number of factors including the proximity of channel walls and the degree of turbulence of the main stream; there will be a critical range of Reynolds number in which this phenomenon takes place, rather than a critical value of the Reynolds number.

Acknowledgement. The author wishes to record his indebtedness to Prof. A. Thom, whose encouragement and advice was of great help throughout this investigation.

LIST OF SYMBOLS

(x, y)	The physical plane
(α, β)	The transformed plane
M	Modulus of transformation from the physical to the α, β plane
ψ	Stream function in viscous flow
ζ	Vorticity
ρ'	Density of the fluid
ν'	Kinematic viscosity
R	Reynolds number
q	Local velocity of flow
u, v	Rectangular components of q
p	Pressure at a point in the fluid
∇^2	Laplacian operator $\left(\frac{\partial^2}{\partial x^2} + \frac{\partial^2}{\partial y^2}\right)$
U'	Velocity of the undisturbed stream
L'	Radius of cylinder

(*Note:* Primed symbols indicate dimensional quantities and unprimed symbols non-dimensional quantities)

REFERENCES

No.	Author	Title, etc.
1	H. Lamb	*Hydrodynamics* (6th Edition). Cambridge University Press. 1932.
2	L. Bairstow, B. M. Cave and E. D. Lang	Two-dimensional slow motion of viscous fluids. *Proc. Roy. Soc.* A. 100. 1922.
3	L. Bairstow, B. M. Cave and E. D. Lang	The resistance of a circular cylinder moving in a viscous fluid. *Phil. Trans. Roy. Soc.* A. 223. 1923.
4	S. Tomotika and T. Aoi ..	The steady flow of a viscous fluid past a sphere and a circular cylinder at small Reynolds numbers. *Quart. J. Mech. App. Math.* III. Pt. 2. June, 1950.
5	A. Thom	The flow past circular cylinders at low speeds. *Proc. Roy. Soc.* A. 141. 1933.
6	M. Kawaguti	Numerical solution of the Navier-Stokes equations for the flow around a circular cylinder at Reynolds number 40. *J. Phys. Soc*, Japan. 8. No. 6. 1953.
7	D. N. de G. Allen and R. V. Southwell	Relaxation methods applied to determine the motion, in two dimensions of a viscous fluid past a fixed cylinder. *Quart. J. Mech. App. Math.* VIII. Part 2. June, 1955.
8	S. Goldstein .. .. .. (editor)	*Modern Developments in Fluid Dynamics.* Oxford University Press. 1938.
9	L. S. G. Kovasznay	Hot wire investigation of the wake behind cylinders at low Reynolds numbers. *Proc. Roy. Soc.* A. 198. 1949.
10	R. B. Payne	Calculations of unsteady viscous flow past a circular cylinder. *J. Fluid Mech.* 4. Pt. 1. May, 1958.
11	L. C. Woods	A note on the numerical solution of fourth-order differential equations. *Aero. Quart.* V. Pt. 3. September, 1954.
12	A. Thom and C. J. Apelt ..	Note on the convergence of numerical solutions of the Navier-Stokes equations. R. & M. 3061. 1956.
13	W. G. Bickley	Finite difference formulae for the square lattice. *Quart. J. Mech. App. Math.* I. Pt. 1. March, 1948.
14	W. G. Bickley	Formulae for numerical differentiation. *Mathematical Gazette.* XXV. No. 263. February, 1941.
15	J. R. Green and R. V. Southwell	Relaxation methods applied to engineering problems.—VIIIA, Problems relating to large transverse displacements of thin elastic plates. *Phil. Trans. Roy. Soc.* A. 239. 1946.

No.	Author	Title, etc.
16	A. Thom and L. Klanfer ..	The method of influence factors in arithmetical solutions of certain field problems. R. & M. 2440. 1947.
17	A. Thom	The arithmetic of field equations. *Aero. Quart.* IV. Pt. 3. August, 1953.
18	A. Fage	Photographs of fluid flow revealed with an ultramicroscope. *Proc. Roy. Soc.* A. 144. 1934.
19	S. Taneda	Experimental investigation of the wake behind cylinders and plates at low Reynolds numbers. *J. Phys. Soc.* Japan. 11. No. 3. 1956.
20	A. Thom	The pressure on the front generator of a cylinder. R. & M. 1389. 1930.
21	G. K. Batchelor	A proposal concerning laminar wakes behind bluff bodies at large Reynolds numbers. *J. Fluid Mech.* I. Pt. 4. October, 1956.
22	C. Camichel, P. Dupin and M. Teissié-Solier	Sur l'existence dans l'ecoulement d'un fluide autour de cylindres immergés, d'un phénomène périodique en régime de Poiseuille. *Comptes Rendus.* 186. 1928.
23	I. Imai	Discontinuous potential flow as the limiting form of the viscous flow for vanishing viscosity. *J. Phys. Soc,* Japan. 8. No. 3. 1953.
24	S. Taneda	Experimental investigation of the wake behind a sphere at low Reynolds numbers. *J. Phys. Soc,* Japan. 11. No. 10. 1956.

APPENDIX I

Accuracy of Solution

Three methods have been employed to check the accuracy of the solution presented here:

(i) *Magnitude of 'Residuals'.* The state of the residuals indicates the internal consistency of the solution, the accuracy with which the finite difference equations are satisfied at each point in the field. By residual is meant, as before, the difference between the recalculated value of ζ or ψ at each point and the previous value. The aim at all times was to reduce the sum of residuals over large areas and at the same time to reduce the average value of each residual. In the present stage of the solution the maximum residual for ζ occurs at the surface of the cylinder and has a value $0{\cdot}066$ where ζ has the value $6{\cdot}238$, and for the half-circumference of the cylinder (19 points) the sum of the residuals of ζ is $-\ 0{\cdot}195$. Since a change of $0{\cdot}0001$ in the value of ψ at a point on the mesh line $\beta = 1$, next to the boundary, will alter the calculated value of ζ at the corresponding point on the boundary by $0{\cdot}012$, the residuals of ζ on the boundary tend to oscillate strongly for very small changes in ψ in the neighbouring field, and their magnitudes should not be taken directly as a measure of the accuracy of the values of ζ on the boundary. From the run of the previous sequences of calculations for boundary values of ζ it is considered that those given in Appendix III are correct, on the whole, in the second decimal place.

In the body of the flow the maximum residual of ζ is approximately $0{\cdot}03$ and except at isolated points the residuals are considerably less than $0{\cdot}01$. The total value of residuals in the area $1 \leqslant \beta \leqslant 20$ (141 points) is $+\ 0{\cdot}042$. It is considered that the present values of ζ are correct in the second decimal place, except perhaps at a few isolated points, and that further refinement of the solution will affect only the third decimal place.

The values of ψ were refined for the present distribution of ζ until for $0 < \beta < 12$ movements in the values of ζ affected only the fourth decimal place and for $\beta > 12$, the third decimal place.

(ii) *The Equation of Continuity.* Across any closed contour in the fluid there must be no net gain or loss of fluid. This check was applied at the same time as the one of the next section. For the solution at the present stage, numerical integration around the circle corresponding to $\beta = 10$ ($r = 4{\cdot}810$) gave a mass inflow of $6{\cdot}960\rho'$ per unit thickness and a mass outflow of $6{\cdot}988\rho'$, giving a discrepancy of $0{\cdot}4$ per cent of either figure. For the circle corresponding to $\beta = 14$ ($r = 9{\cdot}017$) the mass inflow was $12{\cdot}116\rho'$ and the mass outflow $12{\cdot}192\rho'$, a difference of $0{\cdot}6$ per cent.

(iii) *Integrals for Drag.* As was described in the body of the paper, at intervals in the solution the drag force on the cylinder was obtained by integration round several circles enclosing the cylinder and the values obtained were compared with that found by integration round the surface of the cylinder. If X be the force in the x direction applied by the fluid outside the closed contour of integration on the fluid inside the contour, D the drag force on the cylinder (in the x direction) and $G_x^{\cdot}$ the rate of change of momentum of the fluid inside the contour in the x direction, all per unit thickness, then

$$X - D = G_x^{\cdot}. \tag{23}$$

The force X is composed of pressure and friction forces and for integration round a circle of radius r is given by

$$X = -2\int_0^{\pi} p_r \cos\theta \; r\, d\theta - \frac{4}{R}\int_0^{\pi} \zeta_r \sin\theta \; r\, d\theta \,. \tag{24}$$

$G_x^{\cdot}$ is given directly by the net transfer of momentum across the contour in the x direction, since steady conditions are assumed. The values of X and $G_x^{\cdot}$ were found by numerical integration round the circles corresponding to $\beta = 10$ and $\beta = 14$ and the drag force on the cylinder was found by the equation (23).

This check is the most severe of all. To perform the integrations for $G_x^{\cdot}$ and for the first term of the right-hand side of the equation (24) one must first obtain the values of the integrands by numerical differentiation. The process of numerical differentiation is notoriously sensitive to small irregularities in the values of the function being differentiated and, so, very small irregularities in the field will be greatly magnified in the integrals for X and $G_x^{\cdot}$. Further, the term $G_x^{\cdot}$ is given by the difference of two integrations of opposite sign, each very much (20 to 100 times!) greater than the magnitude of $G_x^{\cdot}$ itself. It is to be expected then, and this was found to be the case, that quite small changes in the values of ζ and/or ψ at even a few points near the path of integration will produce large changes in the value of the drag obtained from the equation (23).

For the present solution the drag, expressed as the coefficient C_D, given by integration at the circle $\beta = 10$ was $1{\cdot}14$ and at the circle $\beta = 14$ it was $1{\cdot}52$, compared to the value $1{\cdot}496$ found by integration at the surface of the cylinder.

That the value obtained for C_D by integration around these circles in the fluid is very sensitive to small changes in the configuration of the solution may be illustrated by reference to the values of C_D found by integration at the immediately preceding check. These were:

$$\beta = 10 \qquad C_D = 0{\cdot}91, \quad \beta = 14 \qquad C_D = 1{\cdot}33 \,.$$

The values of ζ at the stage when these integrals were calculated differed from those given in Appendix III by less than $0{\cdot}01$ everywhere and at most points the difference was less than $0{\cdot}005$. Further, the same check applied to Kawaguti's results gave, for integration round a circle of radius $5{\cdot}0$, a value for C_D of $0{\cdot}85$. This is considered to be not so much a criticism of the accuracy of his results as an indication of the extreme severity of this check.

In the light of these remarks and as a result of this and of the preceding checks, it is considered that the numerical results presented in Appendices II and III are of sufficient accuracy for the purposes of this investigation and that further refinement of the solution would result in only slight changes to the numerical results.

APPENDIX II

Reynolds Number 40. ψ *Values*

α \ β	0	1	2	3	4	5	6	7	8	9	10	11	12	13	14	15	16	17	18	19	20
0	0	0	0	0	0	0	0	0	0	0	0	0	0	0	0	0	0	0	0	0	0
1	0	−0·0022	−0·0076	−0·0146	−0·0222	−0·0283	−0·0312	−0·0290	−0·0203	−0·0033	0·0237	0·0624	0·1143	0·180	0·251	0·329	0·418	0·520	0·637	0·773	0·930
2	0	−0·0037	−0·0125	−0·0228	−0·0314	−0·0338	−0·0245	+0·0015	+0·0509	+0·1298	0·2443	0·4004	0·5996	0·845	1·128	1·452	1·847	2·338	2·943	3·715	4·648
3	0	−0·0041	−0·0127	−0·0192	−0·0173	+0·0020	+0·0494	0·1362	0·2763	0·4786	0·7513	1·0994	1·511	1·996	2·530	3·130	3·844	4·700	5·730	6·973	8·461
4	0	−0·0030	−0·0068	−0·0004	+0·0274	0·0910	0·2074	0·3917	0·6554	1·0011	1·4285	1·923	2·478	3·114	3·842	4·690	5·688	6·870	8·275	9·951	11·953
5	0	−0·0004	+0·0063	+0·0363	0·1069	0·2365	0·4424	0·7320	1·1066	1·5562	2·078	2·664	3·341	4·123	5·031	6·091	7·336	8·802	10·533	12·579	—
6	0	+0·0041	0·0275	0·0926	0·2203	0·4257	0·7165	1·0890	1·5358	2·0504	2·640	3·316	4·098	5·005	6·062	7·300	8·750	10·453	12·458	14·821	17·609
7	0	0·0105	0·0573	0·1667	0·3568	0·6310	0·9840	1·4082	1·8998	2·4644	3·112	3·860	4·726	5·732	6·911	8·284	9·898	11·785	14·008	16·615	—
8	0	0·0191	0·0946	0·2518	0·4980	0·8225	1·2136	1·6688	2·1912	2·7913	3·483	4·283	5·210	—	7·553	—	10·757	—	15·157	—	21·214
9	0	0·0293	0·1360	0·3376	0·6255	0·9794	1·3903	1·8620	2·4025	+3·0238	3·743	4·575	—	—	—	—	—	—	—	—	—
10	0	0·0402	0·1769	0·4130	0·7251	1·0916	1·5084	1·9850	2·5305	—	3·888	—	5·714	—	8·193	—	11·578	—	16·211	—	22·557
11	0	0·0510	0·2124	0·4697	0·7901	1·1553	1·5674	2·0368	—	—	—	—	—	—	—	—	—	—	—	—	—
12	0	0·0603	0·2388	0·5032	0·8179	1·1710	1·5679	2·0202	2·5383	—	3·831	—	5·571	—	7·935	—	11·160	—	15·571	—	21·584
13	0	0·0670	0·2527	0·5109	0·8085	1·1400	1·5121	1·9356	—	—	—	—	—	—	—	—	—	—	—	—	—
14	0	0·0696	0·2514	0·4921	0·7639	1·0653	1·4038	1·7890	2·2305	—	3·330	—	4·813	—	6·825	—	9·567	—	13·310	—	18·422
15	0	0·0676	0·2354	0·4493	0·6877	0·9515	1·2478	1·5844	—	—	—	—	—	—	—	—	—	—	—	—	—
16	0	0·0608	0·2059	0·3856	0·5841	0·8040	1·0506	1·3308	1·6519	—	2·451	—	3·529	—	4·991	—	6·983	—	9·700	—	13·411
17	0	0·0497	0·1649	0·3047	0·4581	0·6280	0·8188	1·0353	—	—	—	—	—	—	—	—	—	—	—	—	—
18	0	0·0354	0·1151	0·2105	0·3150	0·4309	0·5607	0·7083	+0·8775	—	1·298	—	1·864	—	2·633	—	3·680	—	5·107	—	7·057
19	0	+0·0184	+0·0591	+0·1074	+0·1603	+0·2188	+0·2849	+0·3595	—	—	—	—	—	—	—	—	—	—	—	—	—
20	0	0	0	0	0	0	0	0	0	0	0	0	0	0	0	0	0	0	0	0	0

APPENDIX III

Reynolds Number 40. ζ *Values*

α \ β	0	1	2	3	4	5	6	7	8	9	10	11	12	13	14	15	16	17	18	19	20
0	0	0	0	0	0	0	0	0	0	0	0	0	0	0	0	0	0	0	0	0	0
1	−0·198	−0·062	0·035	0·108	0·169	0·218	0·260	0·298	0·327	+0·350	+0·365	+0·369	+0·357	0·338	0·315	0·293	0·273	0·256	0·241	0·229	0·218
2	−0·331	−0·088	0·092	0·233	0·351	0·446	0·518	0·571	0·604	0·604	0·574	0·516	0·440	0·358	0·282	0·228	0·180	0·132	0·092	0·050	0·015
3	−0·392	−0·057	0·201	0·404	0·572	0·695	0·763	0·783	0·710	0·585	0·430	+0·240	+0·122	0·010	0	0	0	0	0	0	0
4	−0·362	+0·067	0·399	0·658	0·847	0·930	0·892	0·740	0·505	0·275	+0·070	−0·025	−0·020	0·000	0	0	0	0	0	0	0
5	−0·217	0·304	0·708	0·990	1·109	1·023	0·760	0·459	0·175	+0·030	−0·040	0·000	0	0	0	0	0	0	0	0	0
6	+0·068	0·670	1·109	1·312	1·210	0·870	0·467	0·170	0·015	−0·010	−0·005	0·000	0	0	0	0	0	0	0	0	0
7	0·517	1·180	1·540	1·495	1·076	0·569	0·209	0·047	0·000	−0·005	0	0	0	0	0	0	0	0	0	0	0
8	1·151	1·755	1·882	1·457	0·799	0·299	0·073	0·008	0	0	0	0	0	0	0	0	0	0	0	0	0
9	1·980	2·349	2·060	1·243	0·492	0·125	0·020	0·002	0	0	0	0	0	0	0	0	0	0	0	0	0
10	2·972	2·879	2·049	0·946	0·278	0·044	0·008	0	0	0	0	0	0	0	0	0	0	0	0	0	0
11	4·025	3·263	1·887	0·665	0·134	0·015	0·001	0	0	0	0	0	0	0	0	0	0	0	0	0	0
12	5·019	3·443	1·598	0·420	0·054	0·004	0	0	0	0	0	0	0	0	0	0	0	0	0	0	0
13	5·829	3·409	1·250	0·226	0·017	0·002	0	0	0	0	0	0	0	0	0	0	0	0	0	0	0
14	6·278	3·186	0·957	0·124	0·004	0	0	0	0	r	0	0	0	0	0	0	0	0	0	0	0
15	6·238	2·809	0·705	0·066	0	0	0	0	0	0	0	0	0	0	0	0	0	0	0	0	0
16	5·706	2·340	0·498	0·026	0	0	0	0	0	0	0	0	0	0	0	0	0	0	0	0	0
17	4·741	1·815	0·334	0·009	0	0	0	0	0	0	0	0	0	0	0	0	0	0	0	0	0
18	3·410	1·219	0·201	0·002	0	0	0	0	0	0	0	0	0	0	0	0	0	0	0	0	0
19	+1·796	+0·612	0·094	0	0	0	0	0	0	0	0	0	0	0	0	0	0	0	0	0	0
20	0	0	0	0	0	0	0	0	0	0	0	0	0	0	0	0	0	0	0	0	0

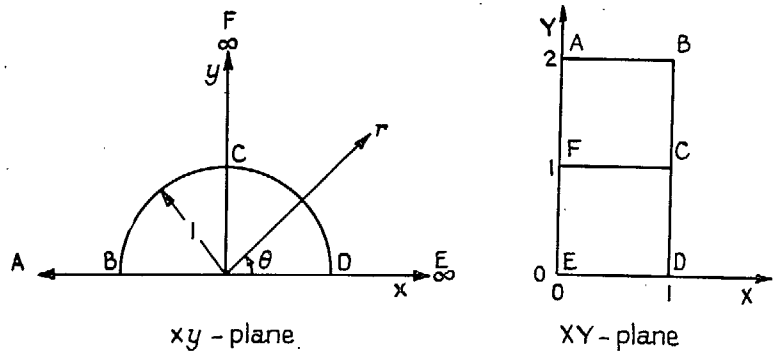

FIG. 1. Transformation, $X = 1/r$, $Y = (2/\pi)\theta$.

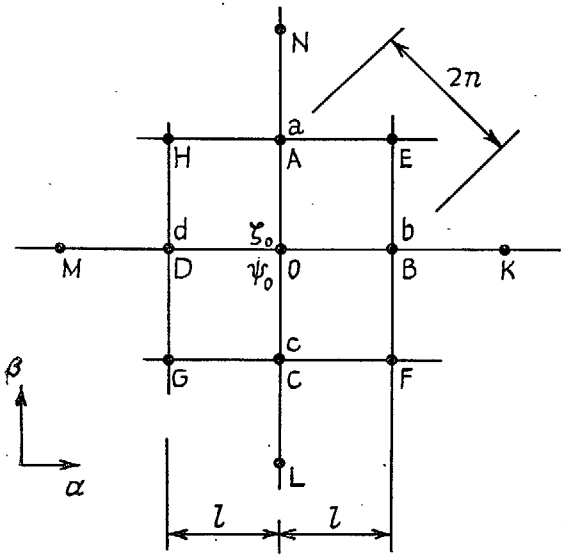

FIG. 3a.

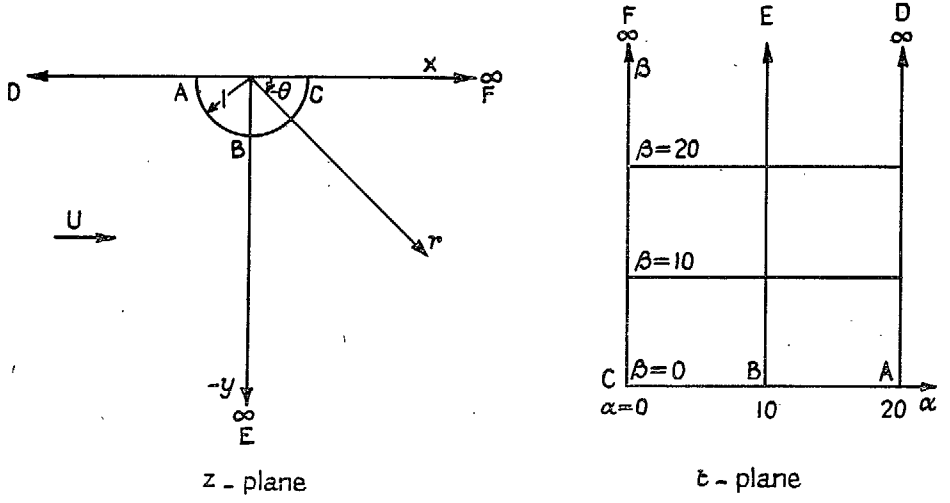

FIG. 2. Transformation, $t = ki \log z$.

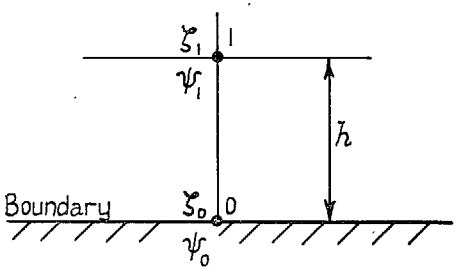

FIG. 3b.

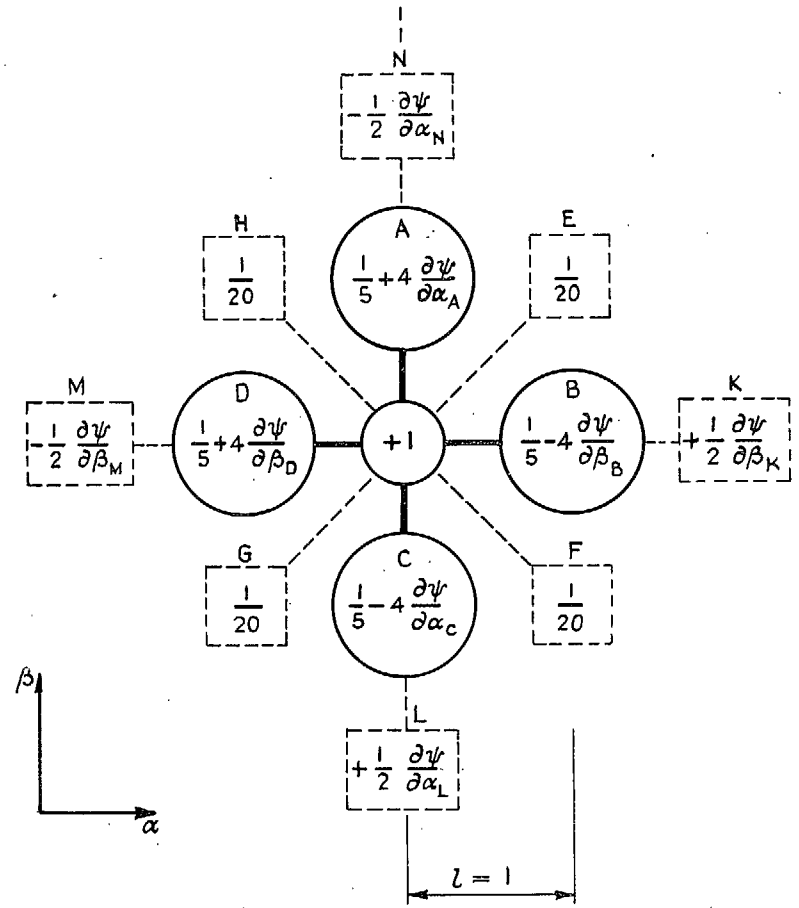

FIG. 4. Unit molecule of operation pattern for ζ.

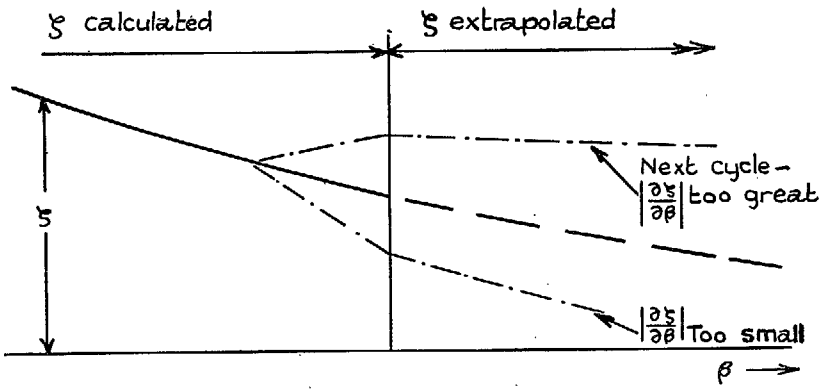

FIG. 5. Extrapolation of ζ in wake.

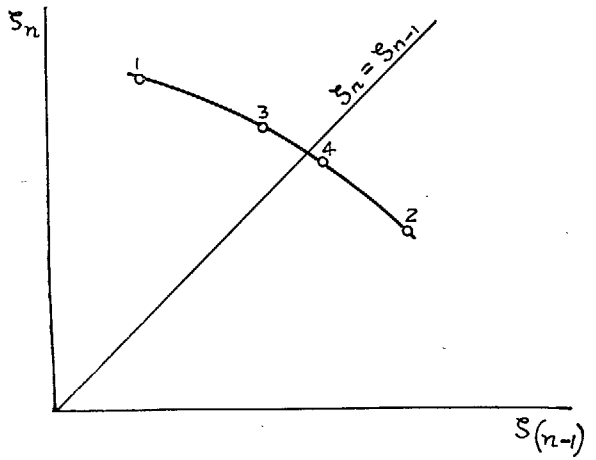

FIG. 6.

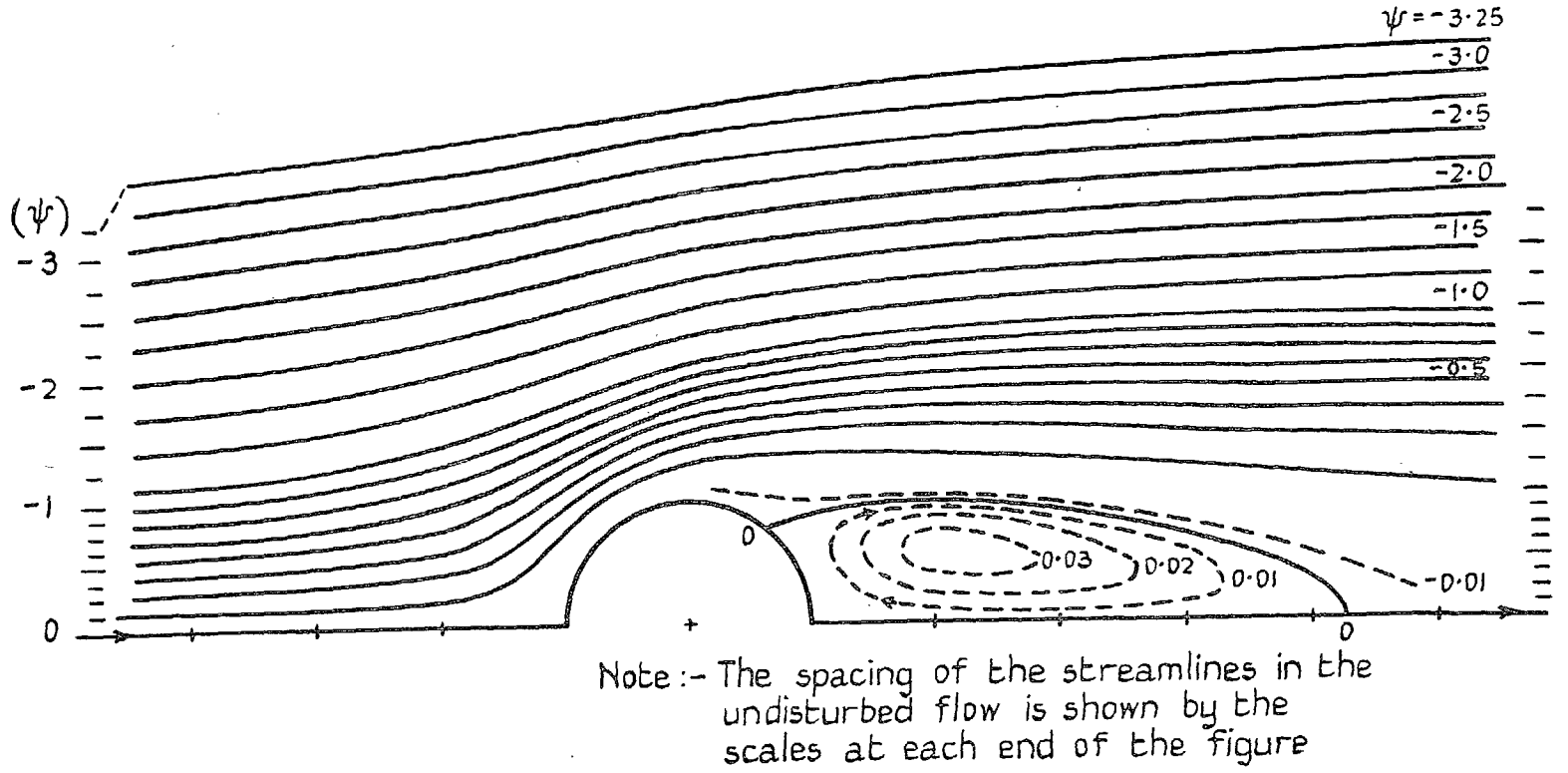

FIG. 7. Calculated streamlines at Reynolds number 40.

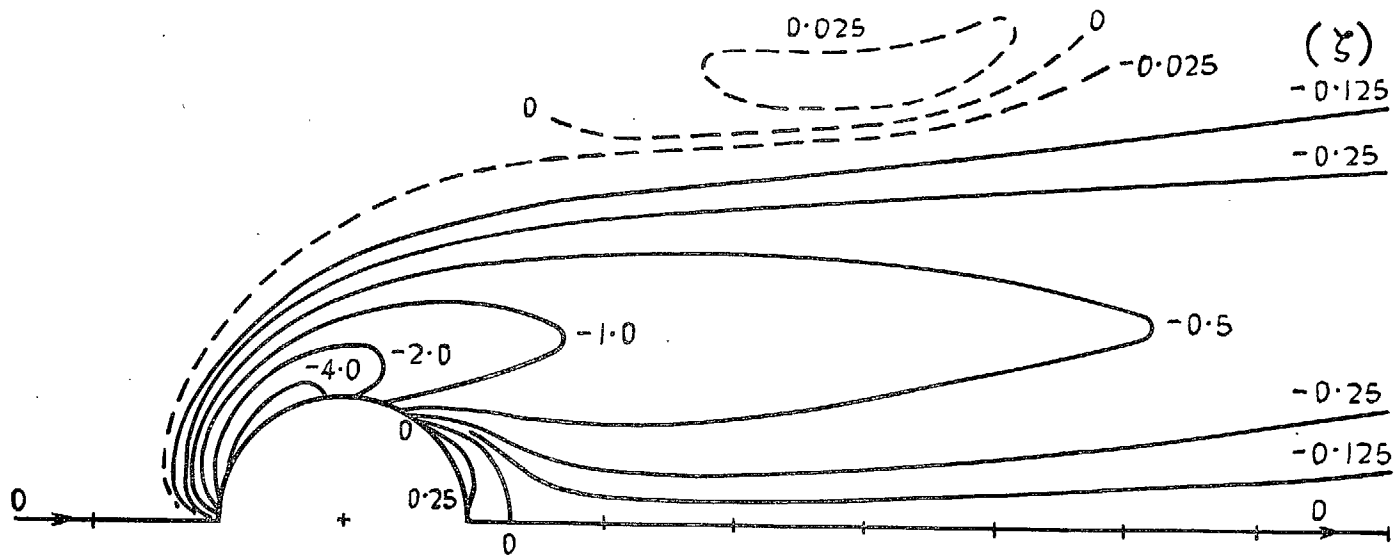

FIG. 8. Equivorticity lines at Reynolds number 40.

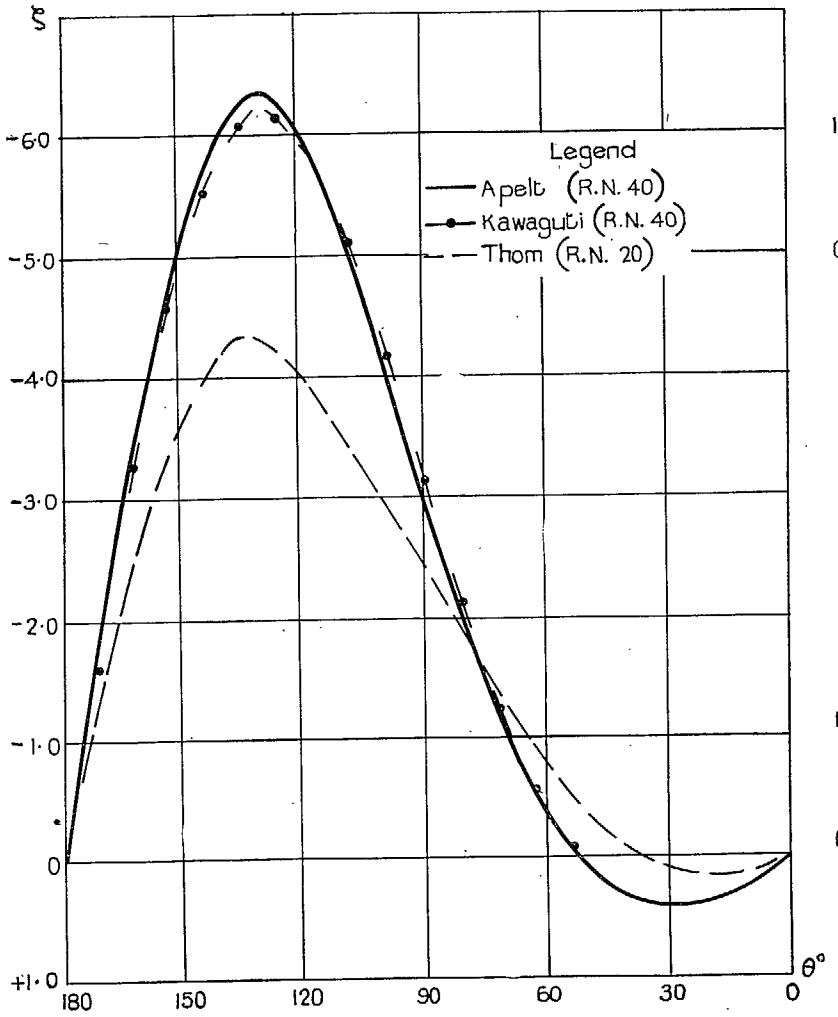

FIG. 9. Vorticity on surface of cylinder.

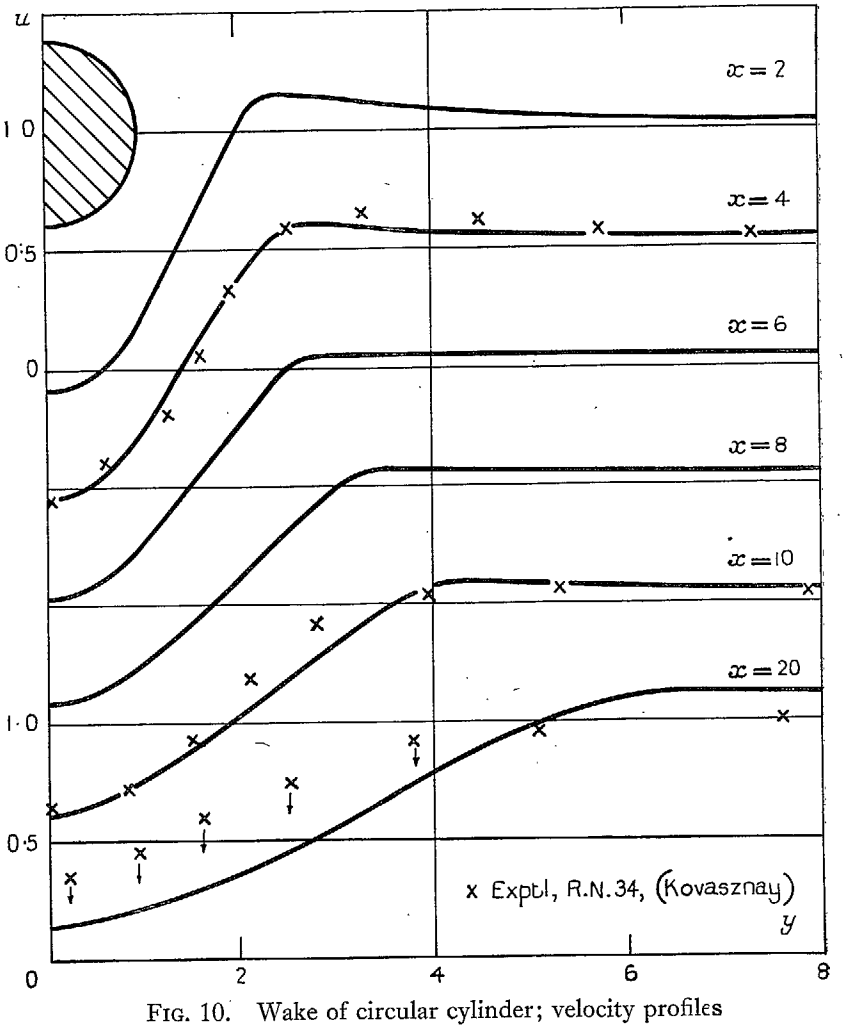

FIG. 10. Wake of circular cylinder; velocity profiles (Reynolds number 40).

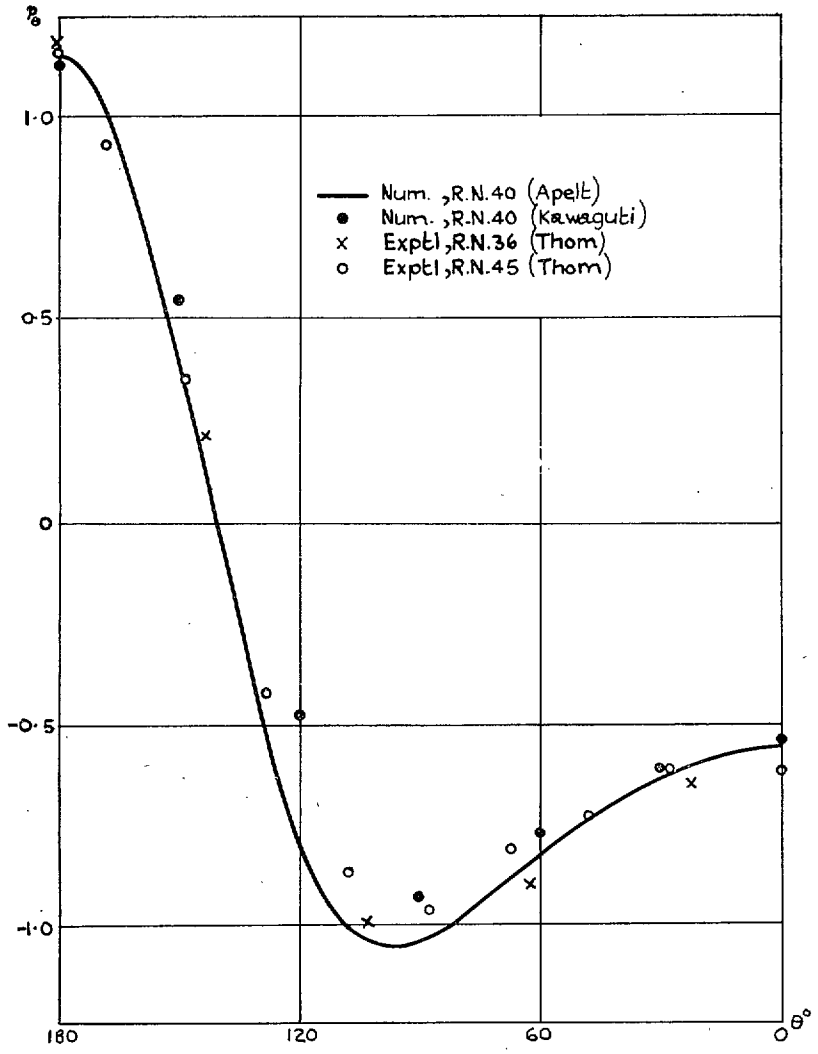

FIG. 11. Pressure on surface of cylinder (Reynolds number 40).

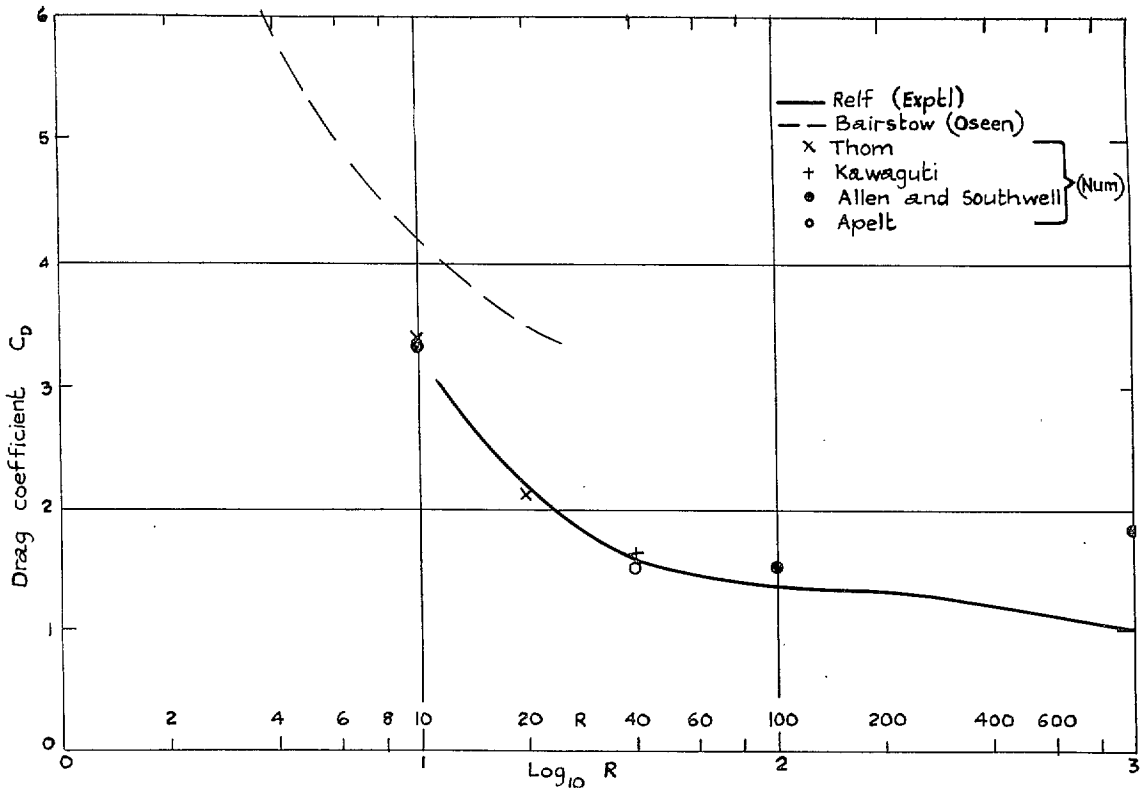

FIG. 12. Drag coefficient of circular cylinder.

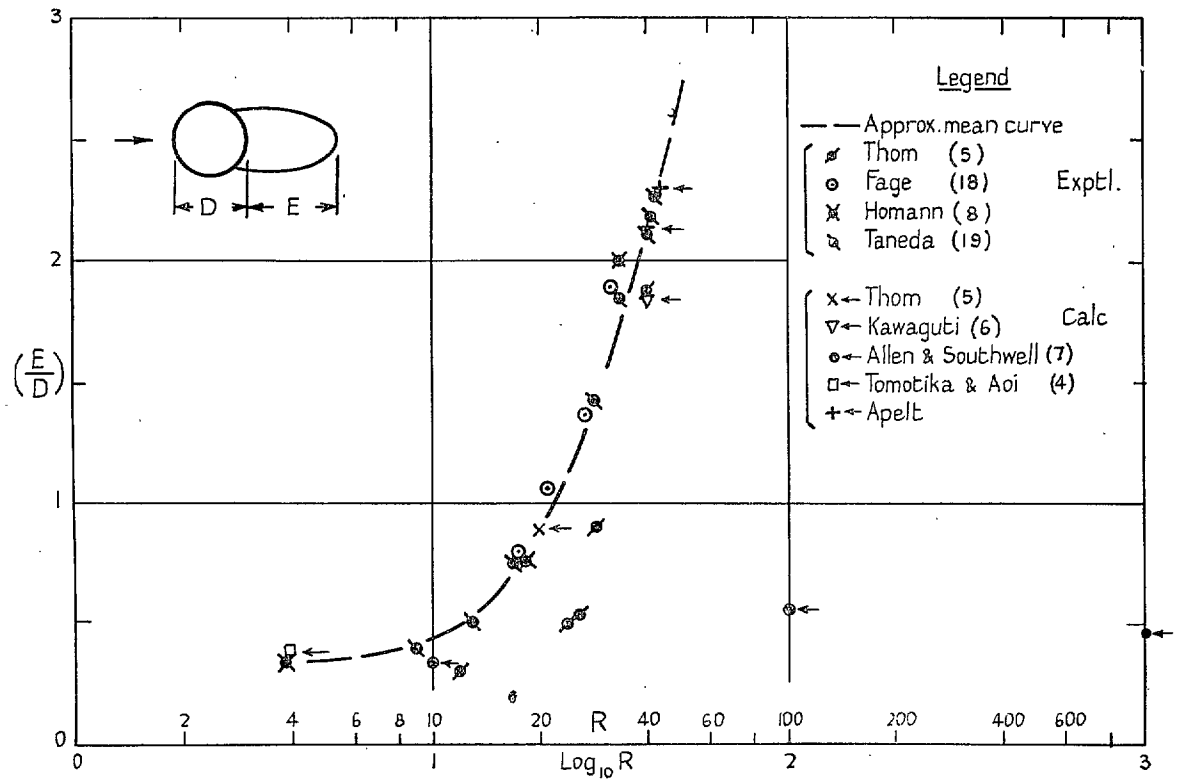

FIG. 13. Standing vortices downstream of circular cylinders.

(79192) Wt. 54/8210 K.5 1/61 Hw.

Publications of the Aeronautical Research Council

ANNUAL TECHNICAL REPORTS OF THE AERONAUTICAL RESEARCH COUNCIL (BOUND VOLUMES)

1941 Aero and Hydrodynamics, Aerofoils, Airscrews, Engines, Flutter, Stability and Control, Structures. 63*s.* (post 2*s.* 3*d.*)

1942 Vol. I. Aero and Hydrodynamics, Aerofoils, Airscrews, Engines. 75*s.* (post 2*s.* 3*d.*)
Vol. II. Noise, Parachutes, Stability and Control, Structures, Vibration, Wind Tunnels. 47*s.* 6*d.* (post 1*s.* 9*d.*)

1943 Vol. I. Aerodynamics, Aerofoils, Airscrews. 80*s.* (post 2*s.*)
Vol. II. Engines, Flutter, Materials, Parachutes, Performance, Stability and Control, Structures. 90*s.* (post 2*s.* 3*d.*)

1944 Vol. I. Aero and Hydrodynamics, Aerofoils, Aircraft, Airscrews, Controls. 84*s.* (post 2*s.* 6*d.*)
Vol. II. Flutter and Vibration, Materials, Miscellaneous, Navigation, Parachutes, Performance, Plates and Panels, Stability, Structures, Test Equipment, Wind Tunnels. 84*s.* (post 2*s.* 6*d.*)

1945 Vol. I. Aero and Hydrodynamics, Aerofoils. 130*s.* (post 3*s.*)
Vol. II. Aircraft, Airscrews, Controls. 130*s.* (post 3*s.*)
Vol. III. Flutter and Vibration, Instruments, Miscellaneous, Parachutes, Plates and Panels, Propulsion. 130*s.* (post 2*s.* 9*d.*)
Vol. IV. Stability, Structures, Wind Tunnels, Wind Tunnel Technique. 130*s.* (post 2*s.* 9*d.*)

1946 Vol. I. Accidents, Aerodynamics, Aerofoils and Hydrofoils. 168*s.* (post 3*s.* 3*d.*)
Vol. II. Airscrews, Cabin Cooling, Chemical Hazards, Controls, Flames, Flutter, Helicopters, Instruments and Instrumentation, Interference, Jets, Miscellaneous, Parachutes. 168*s.* (post 2*s.* 9*d.*)

1947 Vol. I. Aerodynamics, Aerofoils, Aircraft. 168*s.* (post 3*s.* 3*d.*)
Vol. II. Airscrews and Rotors, Controls, Flutter, Materials, Miscellaneous, Parachutes, Propulsion, Seaplanes, Stability, Structures, Take-off and Landing. 168*s.* (post 3*s.* 3*d.*)

Special Volumes

Vol. I. Aero and Hydrodynamics, Aerofoils, Controls, Flutter, Kites, Parachutes, Performance, Propulsion, Stability. 126*s.* (post 2*s.* 6*d.*)

Vol. II. Aero and Hydrodynamics, Aerofoils, Airscrews, Controls, Flutter, Materials, Miscellaneous, Parachutes, Propulsion, Stability, Structures. 147*s.* (post 2*s.* 6*d.*)

Vol. III. Aero and Hydrodynamics, Aerofoils, Airscrews, Controls, Flutter, Kites, Miscellaneous, Parachutes, Propulsion, Seaplanes, Stability, Structures, Test Equipment. 189*s.* (post 3*s.* 3*d.*)

Reviews of the Aeronautical Research Council

1939–48 3*s.* (post 5*d.*) 1949–54 5*s.* (post 5*d.*)

Index to all Reports and Memoranda published in the Annual Technical Reports

1909–1947 R. & M. 2600 6*s.* (post 2*d.*)

Indexes to the Reports and Memoranda of the Aeronautical Research Council

Between Nos. 2351–2449	R. & M. No. 2450 2*s.* (post 2*d.*)
Between Nos. 2451–2549	R. & M. No. 2550 2*s.* 6*d.* (post 2*d.*)
Between Nos. 2551–2649	R. & M. No. 2650 2*s.* 6*d.* (post 2*d.*)
Between Nos. 2651–2749	R. & M. No. 2750 2*s.* 6*d.* (post 2*d.*)
Between Nos. 2751–2849	R. & M. No. 2850 2*s.* 6*d.* (post 2*d.*)
Between Nos. 2851–2949	R. & M. No. 2950 3*s.* (post 2*d.*)

HER MAJESTY'S STATIONERY OFFICE

from the addresses overleaf

Printed and published by
HER MAJESTY'S STATIONERY OFFICE

To be purchased from
York House, Kingsway, London W.C.2
423 Oxford Street, London W.1
13A Castle Street, Edinburgh 2
109 St. Mary Street, Cardiff
39 King Street, Manchester 2
50 Fairfax Street, Bristol 1
2 Edmund Street, Birmingham 3
80 Chichester Street, Belfast 1
or through any bookseller

Printed in England

S.O. Code No. 23-3175